

Cell encapsulation as a tool for stem cell based cell therapy industrialization

Philippe J.R. Cohen, Elisa Luquet, Justine Pletenka, Caroline Royer, Andrea Leonard, Elise Warter, Michele Dai, Basile Gurchenkov, Jessica Carrere, Clément Rieu, Jerome Hardouin, Fabien Moncaubeig, Michael Lanero, Eddy Quelennec, Helene Wurtz, Emilie Jamet, Maelle Demarco, Celine Banal, Paul Van Liedekerke, Pierre Nassoy, Maxime Feyeux, Nathalie Lefort, Kevin Alessandri



Contact: contact@treefrog.fr / www.treefrog.fr

Introduction

Human pluripotent stem cells (hPSCs) have emerged as the most promising cellular source for cell therapies. To overcome the scale-up limitations of classical 2D culture systems, suspension cultures have been developed to meet the need for large-scale culture in regenerative medicine. Despite constant improvements, current protocols that use microcarriers or generate cell aggregates only achieve moderate amplification performance. Here, guided by reports showing that hPSCs can self-organize *in vitro* into cysts reminiscent of the epiblast stage in embryo development, we developed a physio-mimetic approach for hPSC culture. We engineered stem cell niche microenvironments inside microfluidics-assisted core-shell microcapsules. We demonstrate that lumenized three-dimensional colonies significantly improve viability and expansion rates while maintaining pluripotency compared to standard hPSC culture platforms such as 2D cultures, microcarriers, and aggregates. By further tuning capsule size and culture conditions, we scale up this method to industrial-scale stirred tank bioreactors and achieve an unprecedented hPSC amplification rate of 277-fold in 6.5 days. In brief, our findings indicate that our 3D culture system offers a suitable strategy both for basic stem cell biology experiments and for clinical applications.

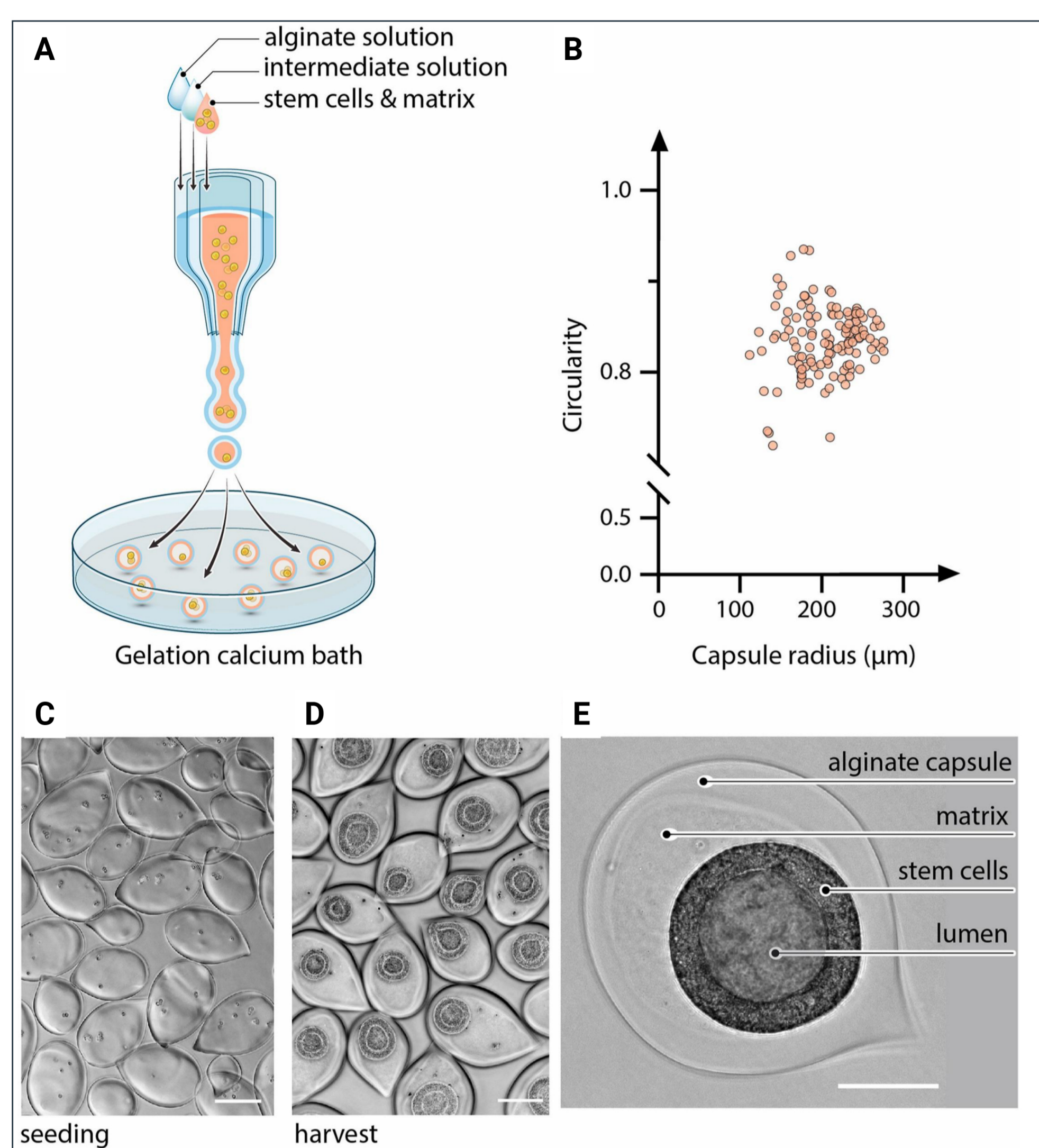


Figure 1. Encapsulation of human pluripotent stem cells (hPSCs) and suspension culture of 3D lumenized colonies (A) Working principle of the microfluidic encapsulation technique. Co-extrusion of three co-axial flows generates composite cell-and extracellular matrix (ECM)-laden droplets. The outer layer composed of alginate solution undergoes gelation upon contact with a calcium bath. Cells are entrapped in the core-shell capsules and ECM condensates onto the internal wall to form a niche-like environment. (B) Morphometric analysis of the capsules. Graph of capsule circularity as a function of capsule radius for a representative batch of capsules ($n = 125$). (C-D) Phase contrast micrographs of the encapsulated hPSCs after seeding at day 0 (C) and before harvest at day 7 (D) of the suspension culture course. Scale bar is 200 μm . (E) Magnified phase contrast image showing the hollow alginate capsule revealing the cyst architecture of the encapsulated hPSC colony. Scale bar = 100 μm .

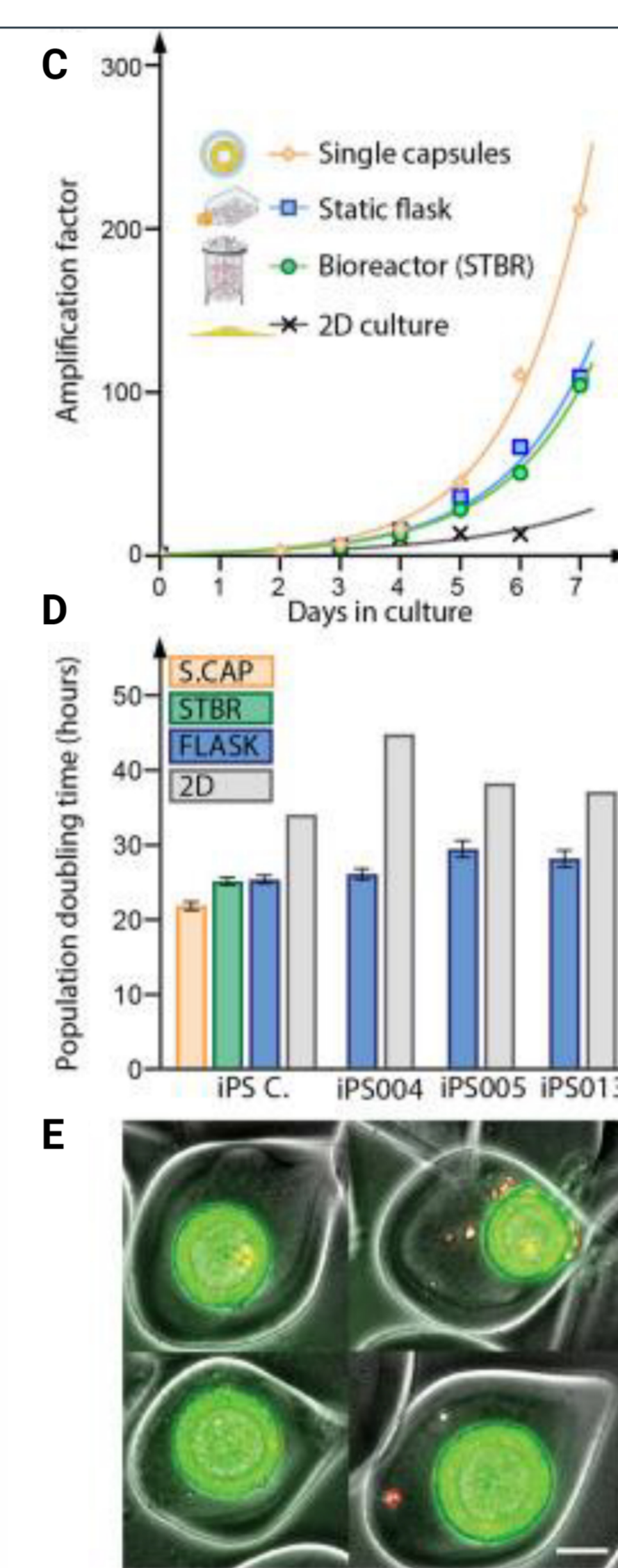
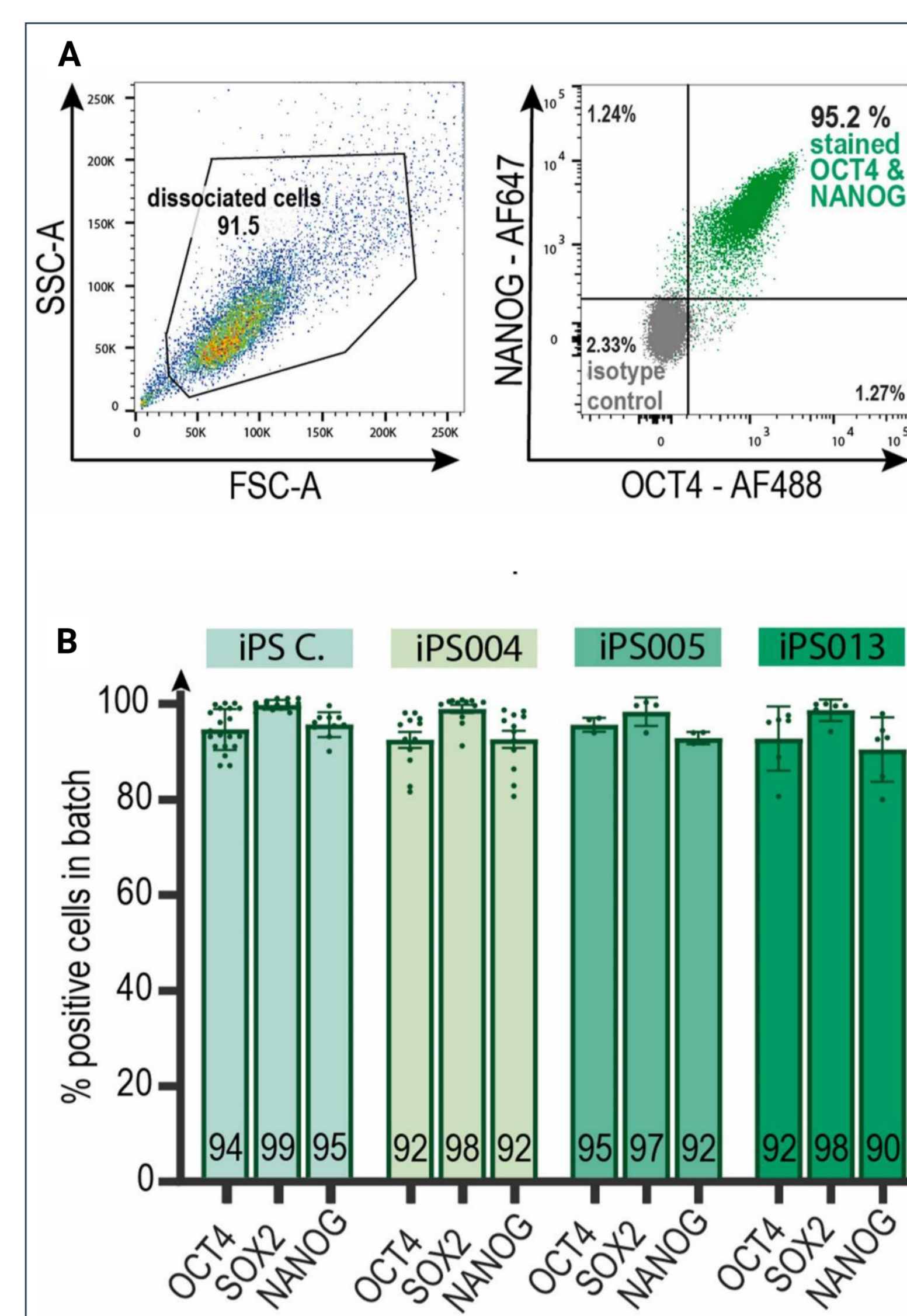


Figure 2. (A) Flow cytometry dot-plots for stemness markers (OCT4 and NANOG) of a batch of 3D hPSC colonies after 7 days of culture (T-flask). (B) Bar chart showing the percentage of OCT4, SOX2 or NANOG positive cells in 3D hPSC colonies (culture in T-flask) analyzed by flow cytometry at 7 days post encapsulation for 4 iPSC cell lines (with $n \geq 3$ independent biological replicates per cell line, $n=42$ total number of experiments). Error bars represent the standard error of the mean. (C) Amplification factor as a function of time for single capsules (orange, $n=6$), static culture (blue, $n=2$), stirred culture in a benchtop (volume 500mL) bioreactor (green, $n=2$), and conventional 2D cultures (grey, $n=1$). Last points in the graph correspond to the harvest time. (D) Population doubling time of encapsulated hPSC colonies in single capsules (S-CAP, orange, $n=6$), in a flask (FLASK, blue, $n=42$), and a benchtop bioreactor (STBR, green, $n=2$) and in standard 2D cultures (2D, grey, $n=1$ for each condition). Error bars represent the standard error of the mean. (E) Fluorescence microscopy image of 4 representative encapsulated 3D hPSC colonies stained with Live/dead (green/red). Scale bar is 100 μm . All data shown here were obtained with iPSC line, except panel 4D which collects data for the 4 available cell lines. (For interpretation of the references to colour in this figure legend, the reader is referred to the Web version of this article.)

Figure 3. Impact of capsule size and oxygen tension on hPSC amplification and scalability in stirred tank bioreactors (A) Phase contrast image showing 3D hPSC colonies in capsules referred to as "big" in the main text (with an average radius of 300 μm). Scale bar = 500 μm . (B) Population doubling time of encapsulated 3D hPSC colonies cultivated in benchtop bioreactors by varying the size of the capsules and the oxygen tension conditions (normoxic versus hypoxic). (C) Picture of a 10 L industrial stirred tank bioreactor used to test the scalability of the stem cell capsule culture system. (D) Graph of amplification factor of hPSCs grown in 10 L bioreactors over a week, in "Big capsules" and hypoxic conditions; Data were obtained from 2 independent batches and from 2 independent encapsulations. Light green band shows the 95% confidence interval of the fitting curve. (For interpretation of the references to colour in this figure legend, the reader is referred to the Web version of this article.)

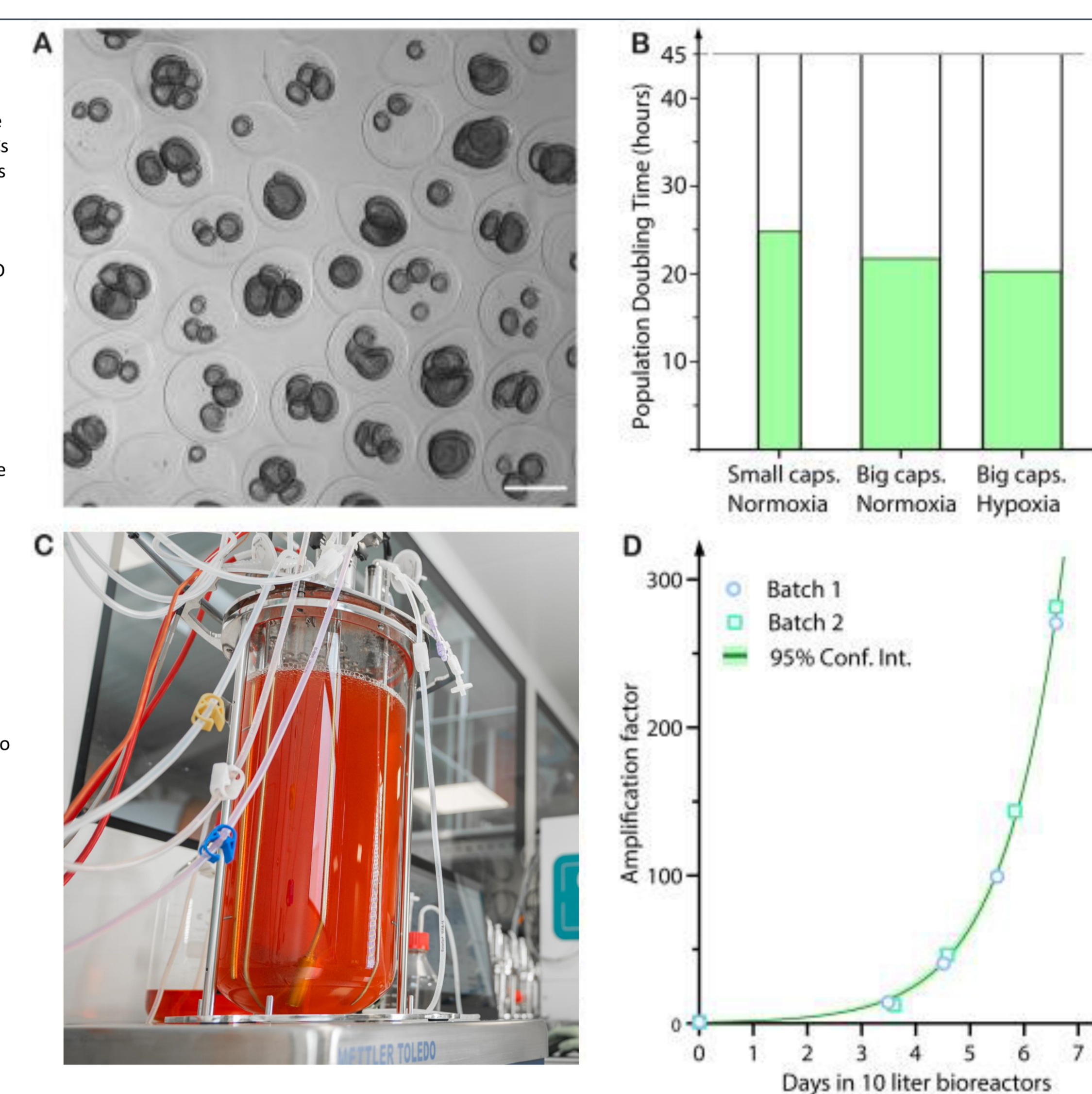


Figure 4. Performance comparison of encapsulator prototype and GMP versions (A) Capsule diameter comparison of encapsulations performed using the large-scale encapsulation device prototype ("Proto") and the GMP compliant version ("GMP"). (B) Cell repartition comparison of encapsulations performed using the large-scale encapsulation device prototype ("Proto") and the GMP compliant version ("GMP"). Readouts performed 30 minutes after encapsulation ($n = 6$ experiments for the "Proto" condition and $n = 5$ experiments for the "GMP" condition); (measurement performed using Amazonia, an in-house developed imaging system, combining a dedicated microscope and a dedicated software suite). Error bars show the standard deviation of the mean. (D) Picture of the "Proto" device in a white, soul crushing, void. (E) Picture of the "GMP" device in a white, soul crushing, void.

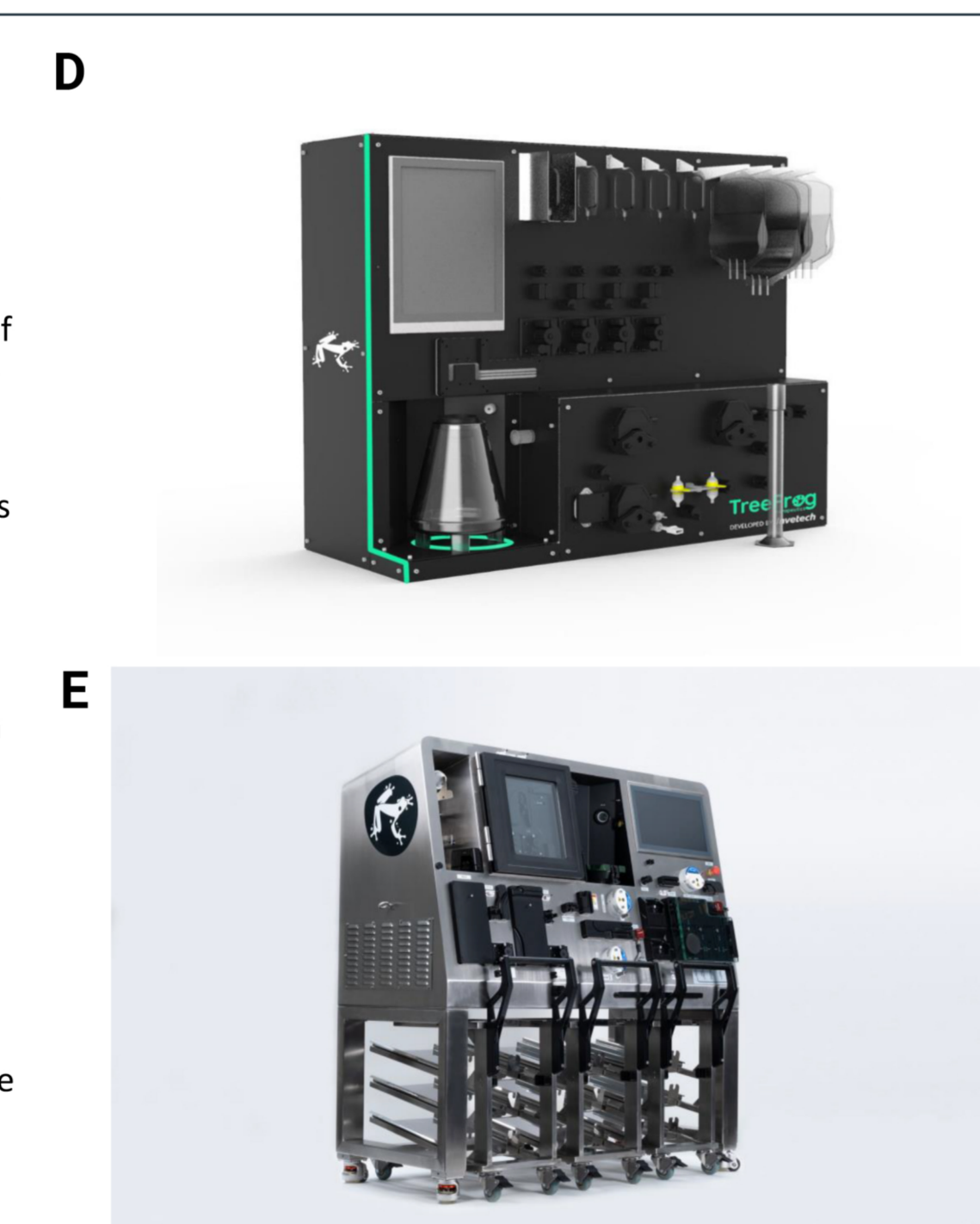
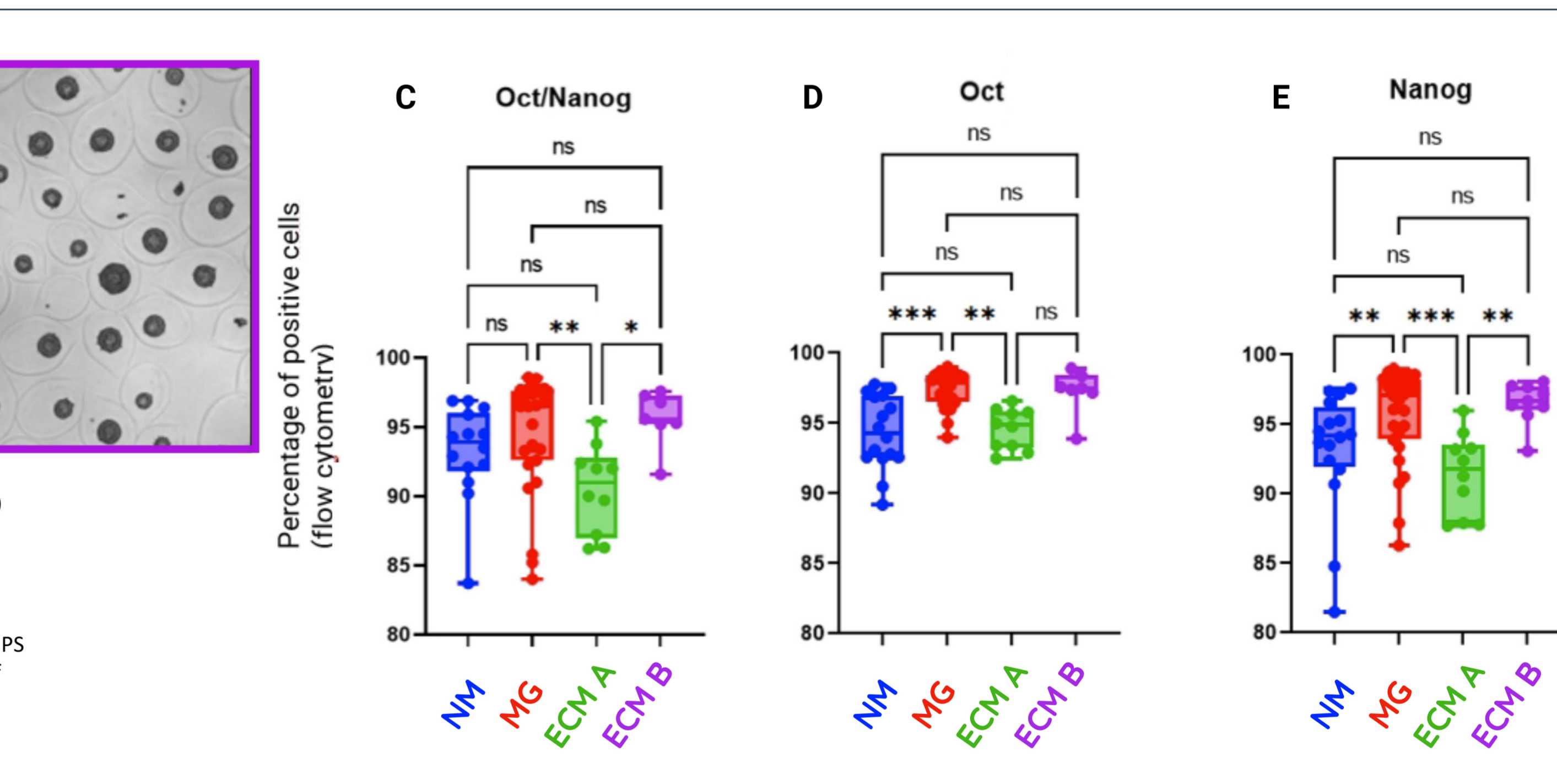


Figure 5. Performance comparison of different matrix compositions within the capsule. (A) Representative picture of pluripotent stem cells encapsulated with ECM A, 5 days after encapsulation, Scale bar is 500 μm . (B) Representative picture of pluripotent stem cells encapsulated with ECM B, 5 days after encapsulation, Scale bar is 500 μm . (C) Bar chart showing the percentage of OCT4 and NANOG dual positive cells in encapsulated 3D hPSC colonies (culture in T-flask) analyzed by flow cytometry at 5 days post encapsulation for 1 iPSC cell line (with $n \geq 7$ independent biological replicates per condition, $n = 55$ total number of experiments).



Conclusion

Hollow alginate capsules with reconstituted niche-like microenvironment can promote the formation and growth of 3D hPSC colonies and provide the necessary protection for scaling up the production in stirred tank bioreactors. Self-organized encapsulated colonies seem to be instrumental for optimal expansion by preserving stem cells' physiological properties. We have demonstrated that our stem cell technology can deliver unprecedented scalability. We anticipate that cell quality is maintained based on extremely high viability, which is taken as a primary signature of cell fitness. Defined matrixes can be substituted to basal membrane extract-based ECMs such as Matrigel™ while enabling higher reproducibility

Perspectives

Future works should focus on assessing the hPSCs quality *in vivo*-like culture systems since the emergence of mutations during culture may be the last limitation to overcome for cell therapy bioproduction.

References

1 P.Cohen et al.2 Alessandri, K., et al. Cellular capsules as a tool for multicellular spheroid production and for investigating the mechanics of tumor progression *in vitro*. Proc Natl Acad Sci 110(37):14843-8 (2013).



This work was supported in part by funding grants from European commission H2020-EIC-SMEInst (grant agreement number: 881,113 C-stemGMP), iLAB2018 Bpi France, Region Nouvelle Aquitaine and Agence Nationale pour la Recherche (ANR-17-C18-0026-02). We acknowledge the Bordeaux Imaging Center, a service unit of the CNRS-INSERM and Bordeaux University, member of the national infrastructure France Biolmaging supported by the French Research Agency (ANR-10-INBS-04). We acknowledge the TBMCore facility. (CNRS UMS 3427 - INSERM US 005). We also thank Nicolas Doulet and Marion Pilorge for helping build the collaboration between Treefrog Therapeutics and the Imagine Institute.